

The connection between star formation and stellar mass: Specific star formation rates to redshift one†‡

Georg Feulner^{1*}, Yuliana Goranova^{1,2}, Niv Drory³, Ulrich Hopp^{1,2},
Ralf Bender^{1,2}

¹ *Universitäts-Sternwarte München, Scheinerstraße 1, D-81679 München, Germany*

² *Max-Planck-Institut für Extraterrestrische Physik, Giessenbachstraße, D-85748 Garching bei München, Germany*

³ *University of Texas at Austin, Austin, Texas 78712*

Accepted 2004 November 23. Received 2004 November 18; in original form 2004 October 6

ABSTRACT

We investigate the contribution of star formation to the growth of stellar mass in galaxies over the redshift range $0.5 < z < 1.1$ by studying the redshift evolution of the specific star formation rate (SSFR), defined as the star formation rate per unit stellar mass. We use an *I*-band selected sample of 6180 field galaxies from the Munich Near-Infrared Cluster Survey (MUNICS) with spectroscopically calibrated photometric redshifts. The SSFR decreases with stellar mass at all redshifts. The low SSFRs of massive galaxies indicates that star formation does not significantly change their stellar mass over this redshift range: The majority of massive galaxies have assembled the bulk of their mass before redshift unity. Furthermore, these highest mass galaxies contain the oldest stellar populations at all redshifts. The line of maximum SSFR runs parallel to lines of constant star formation rate. With increasing redshift, the maximum SFR is generally increasing for all stellar masses, from $\text{SFR} \simeq 5 M_{\odot} \text{yr}^{-1}$ at $z \simeq 0.5$ to $\text{SFR} \simeq 10 M_{\odot} \text{yr}^{-1}$ at $z \simeq 1.1$. We also show that the large SSFRs of low-mass galaxies cannot be sustained over extended periods of time. Finally, our results do not require a substantial contribution of merging to the growth of stellar mass in massive galaxies over the redshift range probed. We note that highly obscured galaxies which remain undetected in our sample do not affect these findings for the bulk of the field galaxy population.

Key words: surveys – galaxies: evolution – galaxies: fundamental parameters – galaxies: mass function – galaxies: photometry – galaxies: stellar content

1 INTRODUCTION

During the last decade, observational research on galaxy formation and evolution made a lot of progress. Especially two quantities and their redshift evolution have gained considerable attention: The stellar mass function of galaxies and the star formation rate (SFR). The stellar mass function was measured out to redshifts of $z \sim 1.5$ (e.g. Bell et al. 2003; Dickinson et al. 2003; Drory et al. 2004; Fontana et al. 2004), while deep pencil beam sur-

veys allowed to trace the SFR to even higher redshifts (e.g. Lilly et al. 1996; Madau et al. 1996, 1998; Steidel et al. 1999; Bouwens et al. 2004; Gabasch et al. 2004).

However, the total integrated SFR and its evolution with redshift does not tell us about the contribution of star formation to the build up of stellar mass for different galaxy masses. For example we cannot say whether the general rise of the SFR to redshift one is produced by high-mass or low-mass galaxies, and how much stellar mass galaxies of different mass form during this period. Cowie et al. (1996) used *K*-band luminosities and [OII] equivalent widths to investigate this connection and noted an emerging population of massive, heavily star forming galaxies at higher redshifts, a phenomenon they termed ‘downsizing’.

A more direct measure of this connection is the ‘specific star formation rate’ (SSFR, Guzman et al. 1997; Brinchmann & Ellis 2000) which is defined as the SFR per unit stellar mass. This quantity allows us to ex-

* E-mail: feulner@usm.lmu.de

† Based on observations collected at the Centro Astronómico Hispano Alemán (CAHA), operated by the Max-Planck-Institut für Astronomie, Heidelberg, jointly with the Spanish National Commission for Astronomy.

‡ Based on observations collected at the VLT (Chile) operated by the European Southern Observatory in the course of the observing proposals 66.A-0123 and 66.A-0129.

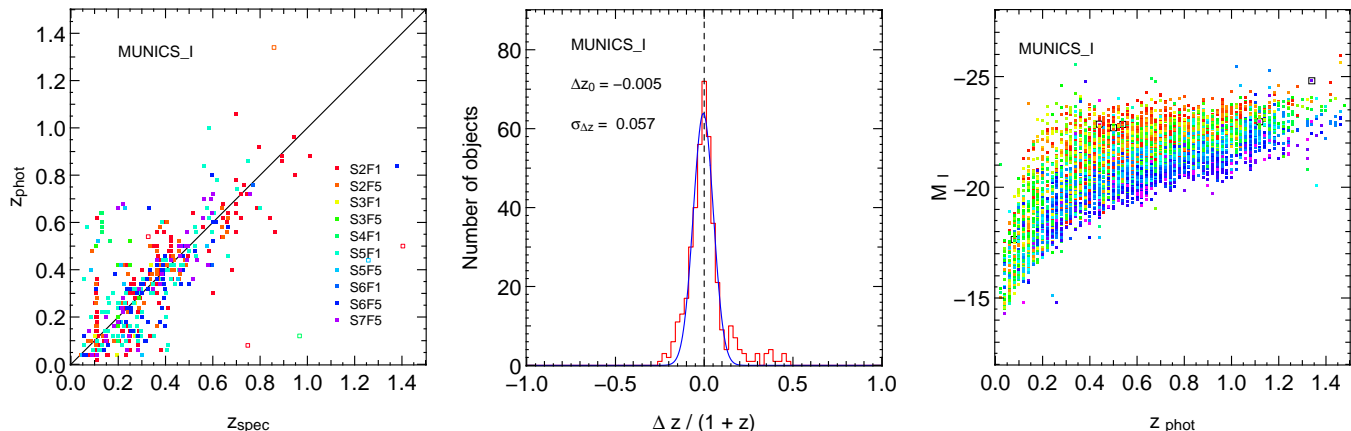


Figure 1. Photometric redshift for the *I*-selected catalogue. The left-hand panel shows a comparison of photometric and spectroscopic redshift for the different MUNICS fields (indicated by the different colours), while the middle panel gives the corresponding error histogram (red) and a Gaussian fit to it (blue). In the right-hand panel we present the distribution of absolute *I* magnitudes M_I versus redshift z_{phot} , where the different colours indicate different model SEDs ranging from early types (red) to late types (purple). Open symbols identify objects spectroscopically classified as AGN.

plore the relation between stellar mass and SFR directly. The SSFR has been studied before, both locally (Pérez-González et al. 2003; Brinchmann et al. 2004) and at higher redshifts (Guzman et al. 1997; Brinchmann & Ellis 2000; Fontana et al. 2003; Bauer et al. 2004). Our study, which relies on photometric redshifts, extends previous work by investigating a large sample of galaxies at higher redshifts.

In this letter, we present measurements of the SSFR and its evolution of redshift based on an *I*-band selected catalogue of more than 6000 field galaxies from the Munich Near-Infrared Cluster Survey (MUNICS), allowing us to trace the change of the SSFR with cosmic time with high statistical accuracy.

This letter is organised as follows. First we introduce the galaxy sample in Section 2 and describe our methods to derive SFRs and stellar masses. In Section 3 we present our results on the SSFR, before we summarise our findings and discuss their implications in Section 4. Throughout this work we assume $\Omega_m = 0.3$, $\Omega_\Lambda = 0.7$ and $H_0 = 70 \text{ km s}^{-1} \text{ Mpc}^{-1}$. All magnitudes are given in the Vega system.

2 THE GALAXY SAMPLE

Galaxies used in this study are drawn from the Munich Near-Infrared Cluster Survey (MUNICS, Drory et al. 2001), a wide-area, medium deep photometric and spectroscopic survey in the *BVRICK* bands covering an area of about 0.3 square degrees down to $K \simeq 19$ and $R \simeq 24$ (Snigula et al. 2002). In contrast to previous work on the *K*-selected sample (“MUNICS_K”, Drory et al. 2001, 2003, 2004), this work is based on an *I*-band selected galaxy catalogue (“MUNICS_I”) which will be described in detail in a forthcoming paper (Feulner et al. 2005, in preparation). Object detection and photometry was performed using YODA (Drory 2003) in much the same way as for the *K*-selected sample (Drory et al. 2001). We use the same sub-set of high-quality fields as in Drory et al. (2001, 2003, 2004). Stars are ex-

cluded based on their spectral energy distributions (SEDs), leaving 6180 galaxies for further analysis.

Photometric redshifts are derived using the method described in Bender et al. (2001). This is the same method also used on MUNICS_K and discussed in detail in Drory et al. (2003). The photometric redshifts are calibrated using the spectroscopic redshifts presented in Feulner et al. (2003). Fig. 1 shows a comparison of photometric and spectroscopic redshifts for MUNICS_I as well as the distribution of absolute *I*-band magnitudes M_I versus redshift. The distribution of redshift errors is similar to MUNICS_K with a width of $\Delta z/(1+z) = 0.057$.

We estimate the star formation rates (SFRs) of our galaxies from the SEDs by deriving the luminosity at $\lambda = 2800 \pm 100 \text{ \AA}$ and converting it to an SFR as described in Madau et al. (1998) assuming a Salpeter initial mass function (IMF; Salpeter 1955). We have convinced ourselves that these photometrically derived SFRs are in reasonable agreement with spectroscopic indicators for objects with available spectroscopy. Note that since our bluest band is *B*, this is an extrapolation for $z < 0.4$. Hence we restrict any further analysis to redshifts $z > 0.4$, where the ultraviolet continuum at $\lambda \simeq 2800 \text{ \AA}$ is shifted into or beyond the *B* band. The SFR density as a function of redshift derived from our sample agrees well with previous results and will be discussed in a future paper (Feulner et al., 2005, in preparation).

Stellar masses are computed from the multi-colour photometry using a method similar to the one used in Drory et al. (2004). It is described in detail and tested against spectroscopic and dynamical mass estimates in Drory, Bender & Hopp (2004). In brief, we derive stellar masses by fitting a grid of stellar population synthesis models by Bruzual & Charlot (2003) with a range of star formation histories (SFHs), ages, metallicities and dust attenuations to the broad-band photometry. We describe star formation histories (SFHs) by a two-component model consisting of a main component with a smooth SFH $\propto \exp(-t/\tau)$ and a burst. We allow SFH timescales $\tau \in [0.1, \infty]$ Gyr, metallicities $[\text{Fe}/\text{H}] \in [-0.6, 0.3]$, ages between 0.5 Gyr and the age of the universe at the objects redshift, and extinctions

$A_V \in [0, 1.5]$. The SFRs derived from this model fitting is in good agreement with the ones from the UV continuum. Note that we apply the extinction correction derived from this fitting also to the SFRs.

3 THE SPECIFIC STAR FORMATION RATE

We investigate the connection between SFR and stellar mass and its evolution with redshift by considering the ‘specific star formation rate’ SSFR (Guzman et al. 1997; Brinchmann & Ellis 2000), defined as the SFR per unit stellar mass. In Fig. 2 we show the SSFR as a function of stellar mass for four different redshift bins from $z = 0.5$ to $z = 1.1$. The general shape is in very good agreement with a similar study based on spectroscopic data (Bauer et al. 2004).

Let us first understand the limits of the object distribution in this diagram as indicated by the dotted lines. First, the sharp cut-off at the high mass end at $\log M_{\text{star}}/M_{\odot} \simeq 11.5$ is produced by the high-mass cut-off of the stellar mass function (see e.g. Drory et al. 2004; Fontana et al. 2004). Secondly, the lower limit at $\log \text{SSFR} \simeq -11.3$ is due to the fact that data points fit by the same model SED occupy horizontal slices in the diagram, with the reddest (oldest, least active) galaxies at the bottom and subsequently bluer models along the distribution to higher values of $\log \text{SSFR}$. Finally, the limit of the point distribution to the left of the diagram is due to a combination of the selection band and the limiting magnitudes in all filters of the MUNICS survey. This completeness limit will run parallel to lines of constant SFR in a B -selected galaxy sample, but have a much steeper slope for near-infrared selected galaxies.

The first result which can be derived from Fig. 2 is that in our optically-selected survey there is an upper bound on the SSFR (with a few galaxies with very high SFRs which are likely starburst galaxies or AGN). It runs parallel to lines of constant star-formation over a wide range of masses $M \gtrsim 10^9 M_{\odot}$ and at all redshifts, meaning that this upper limit of the SFR does not depend on galaxy mass. Furthermore, this maximum SFR is generally increasing with increasing redshift for all stellar masses, from $\text{SFR} \simeq 5 M_{\odot} \text{yr}^{-1}$ at $z \simeq 0.5$ to $\text{SFR} \simeq 10 M_{\odot} \text{yr}^{-1}$ at $z \simeq 1.1$. Note that, while the lower part of the SSFR in the diagram is affected by incompleteness, the constraints on the upper envelope are robust. This is evident from Fig. 3 where we show the histogram of the SFR for the four different redshift bins, clearly showing the increase of the maximum SFR with redshift.

We note that our sample might be missing highly obscured, heavily star forming massive galaxies which could occupy the upper right part of Fig. 2. Indeed, mid-infrared studies have shown that these galaxies exist and that the upper bound of the SSFR is partly a selection effect due to their dust content (Hammer et al. 2001; Franceschini et al. 2003). However, we can conclude from their number density that they contribute at most 10% to the field galaxy population (the objects studied by Franceschini et al. (2003) have 25% of the number density of our sample, but their optical data go roughly 2 mag deeper than ours). Thus, even if our sample should miss these galaxies, our conclusions still hold for the larger part of the field galaxy population. While differences in extinction between galaxies of different mass

might influence the shape of the upper bound, its existence and observed change are robust to these differential effects.

Hints for a shift of this upper envelope to higher SSFRs with redshift were already noted by Brinchmann & Ellis (2000) and Bauer et al. (2004) from smaller galaxy samples, but our large sample of more than 6000 galaxies allows to constrain this change in a much more robust way.

Furthermore, we can study the distribution of the ages of the model stellar populations in Fig. 2. It is clear that the most massive galaxies contain the oldest stellar populations at all redshifts, with ages close to the age of the universe at each epoch.

Finally we indicate the SSFR needed to double a galaxy’s stellar mass between the epoch of observation and today (assuming a constant SFR). Clearly, the most massive galaxies are well below this line at all redshifts, indicating that they formed the bulk of their stars at earlier times, in agreement with the age distribution discussed above. This also means that star formation contributes much more to the mass build-up of less massive galaxies than to high-mass systems. While between redshifts $z = 1$ and $z = 0$ the mass of a $10^{11} M_{\odot}$ system would typically change by $\sim 40\%$ due to star formation, the mass of $10^{10} M_{\odot}$ galaxies would grow by a factor of ~ 5 and that of $10^9 M_{\odot}$ systems by a factor of ~ 40 . This example assumes a constant SFR of $\dot{\rho}_{\star} = 5 M_{\odot} \text{yr}^{-1}$ over a period of 7.7 Gyr which, as will be shown below, is likely to be unrealistic (at least for the lower-mass systems).

4 SUMMARY AND CONCLUSIONS

We have presented the specific star formation rate (SSFR) as a function of stellar mass and redshift for a large sample of more than 6000 I -band selected galaxies. The SSFR decreases with mass at all redshifts, although we might not detect highly obscured galaxies. The low values of the SSFR of the most massive galaxies suggests that most of these massive systems formed the bulk of their stars at earlier epochs. Furthermore, stellar population synthesis models show that these most massive systems contain the oldest stellar populations at all redshifts. This is in agreement with the detection of old, massive galaxies at redshifts $1 \lesssim z \lesssim 2$ (Saracco et al. 2003; Cimatti et al. 2004).

In our optically-selected sample, there is an upper bound to the SSFR of the majority of field galaxies which is parallel to lines of constant star formation rate (SFR). This upper limit on the SFR is independent of stellar mass, but increases with redshift from $\text{SFR} \simeq 5 M_{\odot} \text{yr}^{-1}$ at $z \simeq 0.5$ to $\text{SFR} \simeq 10 M_{\odot} \text{yr}^{-1}$ at $z \simeq 1.1$.

We can also infer from Fig. 2 that star formation in lower mass galaxies cannot proceed at constant SFR for a long time: All galaxies above the dot-dashed line in the diagram have the potential to double their stellar mass between the epoch of observation and today (assuming a constant SFR). While lower mass galaxies at low redshift tend to be gas rich, there is a large spread in measured gas-to-stellar-mass fractions (Mateo 1998; Pérez-González et al. 2003; Kannappan 2004). However, very gas-rich systems are rare (Davies et al. 2001), i.e. the majority of these galaxies does not have huge gas supplies, which might lead us to believe that low-mass galaxies cannot exhibit constant star formation over longer time-scales, but show variable star for-

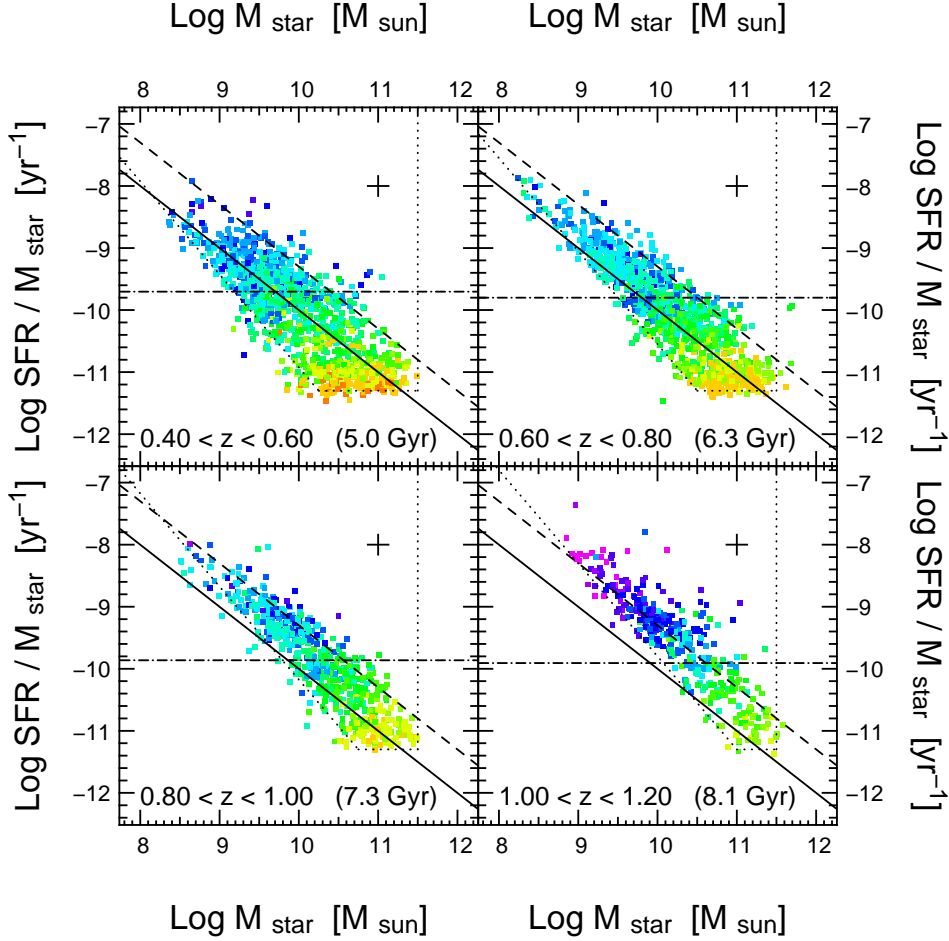


Figure 2. The SSFR as a function of stellar mass for MUNICS-I. The solid and dashed lines correspond to SFRs of $1 M_{\odot} \text{ yr}^{-1}$ and $5 M_{\odot} \text{ yr}^{-1}$, respectively. While this is a good measure of the upper envelope of the majority of objects at $z \sim 0.5$, the point distribution shifts to higher SSFRs with increasing redshift. The dotted lines indicate the limits of the point distribution due to magnitude limits, the model SED set and the mass function (see the text for details). Objects are coloured according to the age of the CSP model fit to the photometry, ranging from 9 Gyr (red) to 0.05 Gyr (purple). The dot-dashed line is the SSFR required to double a galaxy’s mass between each redshift epoch and today (assuming constant SFR); the corresponding look-back time is indicated in each panel. The error cross in each panel gives an idea of the typical errors.

mation histories, like the ones derived for the – even lower mass – dwarf galaxies in the Local Group (see e.g. Mateo 1998; Tosi 2001; Grebel 2004 for reviews). Due to the degeneracy of different star formation histories in colour space, it is not possible to say from our data whether we see these galaxies in the process of formation or during one of multiple episodes of active star formation. However, it is likely that we pick them up during an active phase of star formation. Also, it is clear from the completeness limits that we cannot detect low-mass galaxies with low SSFR.

Considering the high-mass end, we can try to draw some conclusions about the contributions of star formation and merging to the change of stellar mass. Between redshifts $z \simeq 1.1$ and $z \simeq 0.5$, the characteristic mass of the cut-off of the galaxies’ stellar mass function changes by $\Delta \log M \simeq 0.15$ dex (Drory et al. 2004; Fontana et al. 2004; Conselice et al. 2004). For a $M_{\star} = 10^{11} M_{\odot}$ stellar mass galaxy, a constant SFR of $\dot{\rho}_{\star} = 5 M_{\odot} \text{ yr}^{-1}$ over a period of time of $\Delta t = 3.1$ Gyr (the difference in time between these redshift values), yields a growth in stellar mass of $\Delta M_{\star} \simeq 2 \cdot 10^{10} M_{\odot}$, or $\Delta \log M_{\star} \simeq 0.1$ dex. Consider-

ing the uncertainty of the results and our lack of knowledge about the star formation histories of these galaxies, we cannot really decide about the relative importance of star formation and merging. We note, however, that our results on the growth of stellar mass in massive galaxies does not require a substantial contribution of merging over the redshift range $0 \lesssim z \lesssim 1$.

Overall it is clear that there is a marked difference between the star formation histories of low-mass and high-mass galaxies in agreement with findings from the stellar populations of today’s galaxies (Heavens et al. 2004; Thomas et al. 2004).

ACKNOWLEDGMENTS

We thank the anonymous referee for his comments which helped to improve the presentation of this letter. The authors would like to thank the staff at Calar Alto Observatory for their support. Furthermore, we thank Amanda Bauer for discussion and Jan Snigula for help with the colour figures.

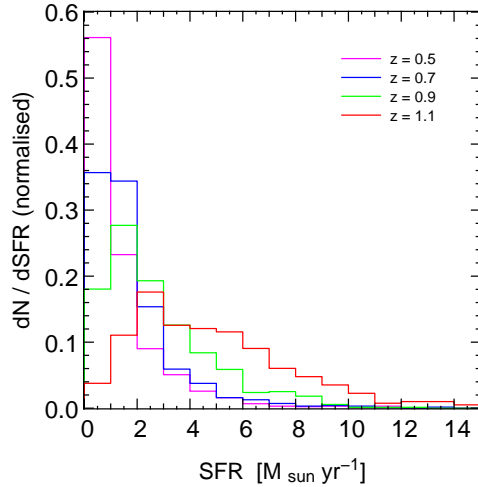


Figure 3. Normalised histogram of the SFR for the four different redshift bins. The shift of the high-SFR cut-off to higher SFRs with increasing redshift is clearly visible. The individual histograms are divided by the number of objects in each redshift bin. Note that at higher redshifts incompleteness starts to cut away objects with low SFR as indicated in Fig. 2.

We acknowledge funding by the DFG (SFB 375). This research has made use of NASA’s Astrophysics Data System (ADS) Abstract Service.

REFERENCES

- Bauer A., Drory N., Hill G. J., Feulner G., 2004, *ApJ*, submitted
- Bell E. F., McIntosh D. H., Katz N., Weinberg M. D., 2003, *ApJS*, 149, 289
- Bender R., et al., 2001, in Cristiani S., Renzini A., Williams R. E., eds, *Deep Fields The FORS Deep Field: Photometric Data and Photometric Redshifts*. Springer, p. 96
- Bouwens R. J., Illingworth G. D., Thompson R. I., Blakeslee J. P., Dickinson M. E., Broadhurst T. J., Eisenstein D. J., Fan X., Franx M., Meurer G., van Dokkum P., 2004, *ApJ*, 606, L25
- Brinchmann J., Charlot S., White S. D. M., Tremonti C., Kauffmann G., Heckman T., Brinkmann J., 2004, *MNRAS*, 351, 1151
- Brinchmann J., Ellis R. S., 2000, *ApJ*, 536, L77
- Bruzual G., Charlot S., 2003, *MNRAS*, 344, 1000
- Cimatti A., Daddi E., Renzini A., Cassata P., Vanzella E., Pozzetti L., Cristiani S., Fontana A., Rodighiero G., Mignoli M., Zamorani G., 2004, *Nat*, 430, 184
- Conselice C. J., et al., 2004, *ApJ*, submitted, astro-ph/0405001
- Cowie L. L., Songaila A., Hu E. M., Cohen J. G., 1996, *AJ*, 112, 839
- Davies J. I., de Blok W. J. G., Smith R. M., Kambas A., Sabatini S., Linder S. M., Salehi-Reyhani S. A., 2001, *MNRAS*, 328, 1151
- Dickinson M., Papovich C., Ferguson H. C., Budavári T., 2003, *ApJ*, 587, 25
- Drory N., 2003, *A&A*, 397, 371
- Drory N., Bender R., Feulner G., Hopp U., Maraston C., Snigula J., Hill G. J., 2003, *ApJ*, 595, 698 (MUNICS II)
- Drory N., Bender R., Feulner G., Hopp U., Maraston C., Snigula J., Hill G. J., 2004, *ApJ*, 608, 742 (MUNICS VI)
- Drory N., Bender R., Hopp U., 2004, *ApJ*, 616, L106
- Drory N., Bender R., Snigula J., Feulner G., Hopp U., Maraston C., Hill G. J., Mendes de Oliveira C., 2001, *ApJ*, 562, L111 (MUNICS III)
- Drory N., Feulner G., Bender R., Botzler C. S., Hopp U., Maraston C., Mendes de Oliveira C., Snigula J., 2001, *MNRAS*, 325, 550 (MUNICS I)
- Feulner G., Bender R., Drory N., Hopp U., Snigula J., Hill G. J., 2003, *MNRAS*, 342, 605 (MUNICS V)
- Fontana A., Donnarumma I., Vanzella E., Giallongo E., Menci N., Nonino M., Saracco P., Cristiani S., D’Odorico S., Poli F., 2003, *ApJ*, 594, L9
- Fontana A., Pozzetti L., Donnarumma I., Renzini A., Cimatti A., Zamorani G., Menci N., Daddi E., Giallongo E., Mignoli M., Perna C., Salimbeni S., Saracco P., Broadhurst T., Cristiani S., D’Odorico S., Gilmozzi R., 2004, *A&A*, 424, 23
- Franceschini A., Berta S., Rigopoulou D., Aussel H., Cersasky C. J., Elbaz D., Genzel R., Moy E., Oliver S., Rowan-Robinson M., Van der Werf P. P., 2003, *A&A*, 403, 501
- Gabasch A., Salvato M., Saglia R. P., Bender R., Hopp U., Seitz S., Feulner G., Pannella M., Drory N., Schirmer M., Erben T., 2004, *ApJ*, 616, L83
- Grebel E. K., 2004, in *Origin and Evolution of the Elements The Evolutionary History of Local Group Irregular Galaxies*. p. 237
- Guzman R., Gallego J., Koo D. C., Phillips A. C., Lowenthal J. D., Faber S. M., Illingworth G. D., Vogt N. P., 1997, *ApJ*, 489, 559
- Hammer F., Gruel N., Thuan T. X., Flores H., Infante L., 2001, *ApJ*, 550, 570
- Heavens A., Panter B., Jimenez R., Dunlop J., 2004, *Nat*, 428, 625
- Kannappan S. J., 2004, *ApJ*, 611, L89
- Lilly S. J., Le Fèvre O., Hammer F., Crampton D., 1996, *ApJ*, 460, L1
- Madau P., Ferguson H. C., Dickinson M. E., Giavalisco M., Steidel C. C., Fruchter A., 1996, *MNRAS*, 283, 1388
- Madau P., Pozzetti L., Dickinson M., 1998, *ApJ*, 498, 106
- Mateo M. L., 1998, *ARA&A*, 36, 435
- Pérez-González P. G., Gil de Paz A., Zamorano J., Gallego J., Alonso-Herrero A., Aragón-Salamanca A., 2003, *MNRAS*, 338, 525
- Salpeter E. E., 1955, *ApJ*, 121, 161
- Saracco P., Longhetti M., Severgnini P., Della Ceca R., Mannucci F., Bender R., Drory N., Feulner G., Ghinassi F., Hopp U., Maraston C., 2003, *A&A*, 398, 127
- Snigula J., Drory N., Bender R., Botzler C. S., Feulner G., Hopp U., 2002, *MNRAS*, 336, 1329 (MUNICS IV)
- Steidel C. C., Adelberger K. L., Giavalisco M., Dickinson M., Pettini M., 1999, *ApJ*, 519, 1
- Thomas D., Maraston C., Bender R., Mendes de Oliveira C., 2004, *ApJ*, in press, astro-ph/0410209
- Tosi M., 2001, in *Dwarf galaxies and their environment Stellar Populations and Chemical Evolution of Late-Type Dwarf Galaxies*. p. 67